



Nineteenth European Conference on Chemical Vapor Deposition, (EUROCV D 19)

The influence of F-doping in SnO₂ thin films

H.M. Yates^{a1}, P. Evans^a, D.W. Sheel^{a, b},

^aMaterials and Physics Research Centre, University of Salford, Manchester, M5 4WT, UK

^bCVD Technologies Ltd., University of Salford Campus, Manchester, M5 4WT, UK

Abstract

Transparent conductive oxide (TCO) films are widely used in many consumer products. The properties of the TCO can critically affect the efficiency of the application. With this in mind the surface morphological, optical and electrical properties have been targeted by systematic exploration of the Atmospheric Pressure Chemical Vapour Deposition (APCVD) growth parameters and in this work particularly the effect of dopant concentrations. APCVD processes are particularly suited to use in industry due to the high volume, continuous growth processes and fast growth rates achievable. Using the APCVD process, F-doped SnO₂ has been deposited on glass using monobutyl tin trichloride with trifluoro-acetic acid as the dopant source. The deposited films were characterised for crystallinity, morphology, optical haze and electrical properties. Additionally, the stability of the films to post growth annealing were studied, as this is an important factor as most TCO's will need further processing for the production of consumer products. It has been shown that increasing the dopant levels led to a decrease in surface roughness along with a reduction in feature size. The surface features also showed a decrease in the average angle, although with a broader distribution. As expected increased doping gave increased carrier concentration and mobility, with a non-linear decrease in resistivity. The polycrystalline structure became less selective in orientation on doping, but no further change was seen on increasing the dopant level. The samples tested showed only marginal changes in electrical and optical properties at elevated temperatures, confirming their thermal stability.

© 2013 The Authors. Published by Elsevier B.V. Open access under [CC BY-NC-ND license](https://creativecommons.org/licenses/by-nc-nd/4.0/).
Selection and peer-review under responsibility of Organizing Committee of EUROCV D 19.

Keywords: tin oxide; atmospheric pressure chemical vapour deposition; F-dopant;

* Corresponding author. Tel.: +44-161-295-3115; fax: +44-161-295-5575.
E-mail address: H.M.Yates@Salford.ac.uk.

1. Introduction

Transparent conductive oxide (TCO) films are of high importance in today's society with wide ranging application to many consumer products [1,2] such as flat screen high-definition televisions, energy efficient windows and thin film photovoltaic cells [3]. The properties of the TCO can critically affect final product performance. The exact properties required depend on the application, so an ability to easily tailor the film properties without resort to alternative production methods is advantageous. Atmospheric Pressure Chemical Vapour Deposition (APCVD) is often attractive for this purpose, as by careful choice of the deposition parameters the film properties can be systematically targeted. Use of APCVD on the lab-scale has direct relevance to that in industry as the technology has been proven to be capable of transfer to batch or roll-to-roll production lines. The technique has the potential for substantial cost reduction due to low material consumption, reduced running costs (compared to low pressure systems) and high deposition rates.

We have previously demonstrated the ability of this technique to produce TCO's with high optical haze and transparency suitable for solar cells [4], as well as those with high transparency, low optical haze and low emissivity suitable for energy efficient windows [5]. Earlier research by this group with F-doped SnO₂ established that the film morphology, along with its optical and electrical properties could be modified by use of different APCVD parameters such as deposition time [6], tin precursor [7], additives [8,9], temperature or growth rate [10].

In this paper we have explored the effects of the F-dopant on the film properties.

2. Experimental Details

2.1. TCO growth

The SnO₂:F thin films were deposited by APCVD at 600 °C using monobutyl tin trichloride (5.72×10^{-4} mol min⁻¹) with a Sn precursor to H₂O molar ratio of 5:1. The dopant, Trifluoro-acetic acid (TFAA) was added with the water at a range of concentrations. Nitrogen was used as the carrier gas, with 20% oxygen at a total flow of 2 l/min. Deposition was on 1 mm thick borosilicate (Corning Eagle 2000) glass. An APCVD gas handling system combined with an in-house designed coater head system was employed to deliver precursors to the surface of the substrate. On this system the heated substrate is translated on an automated stage, beneath a static, non-contact gas distributor in an extracted, open atmosphere, enclosure. The number of substrate passes under the CVD coating head was adjusted to maintain constant film thickness. Details of the equipment have previously been published [10].

2.2. Characterisation

The crystallinity and structure of the samples was assessed by X-ray diffraction (Siemens D5000). The morphology and surface roughness of the samples was obtained by atomic force microscopy (NanoScope IIIa, Digital Inst. Ltd). Film thickness was measured using a Dektak 3ST surface profiler on an etched step edge. Hall Effect measurements were performed on the SnO₂:F films to determine the electrical properties with a lab built system using an electromagnetic with a magnetic flux density of 0.84 T. Reflectance and

transmittance were measured on a spectrophotometer (nkd8000, Aquila Instruments Ltd) with p-polarised light at an incident angle of 30°.

3. Results and Discussion

All samples were of similar thickness, 1.8 μm , to reduce the difficulties of comparison, as thickness has a strong effect on many film properties such as electrical resistance and surface roughness. From Table 1 it can be seen that there was a reduction in growth rate as the dopant concentration increased. This behaviour has been reported previously for deposition of $\text{SnO}_2\text{:F}$ by Plasma Enhanced CVD [11] and spray-deposited films [12,13]. The reduction in growth rate has been ascribed to etching of the growing surface by HF which is one of the gaseous reaction products.

Table 1. Sample dopant levels, growth rate and surface roughness

TFAA doping (M)	Thickness (nm)	Growth (rate, nm/pass)	Roughness (nm)
0	1840	131	75
0.05	1746	125	-
0.1	1806	129	78
0.2	1850	103	55
0.4	1760	98	44
0.6	1793	90	45

There was a non-linear trend of reducing roughness (RMS) as the dopant levels increased. Atomic Force Microscopy (AFM) images showed a reduction in feature size at higher dopant levels, as shown in figure 1. Previous research also reported reduction in feature size of SnO_2 films with increasing levels of a Sb dopant, although no reason was given [14]. Earlier work by us, using the same deposition process, established that lower growth rates reduced the variation of in feature height [10]. The actual shape of the feature showed no obvious changes as viewed from the images.

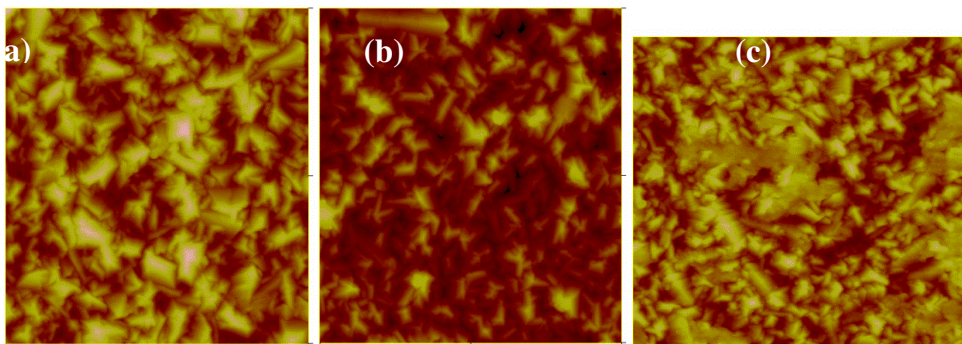


Fig. 1. AFM images (5 μm x 5 μm) of (a) no dopant, (b) 0.1M TFAA, (c) 0.6M TFAA

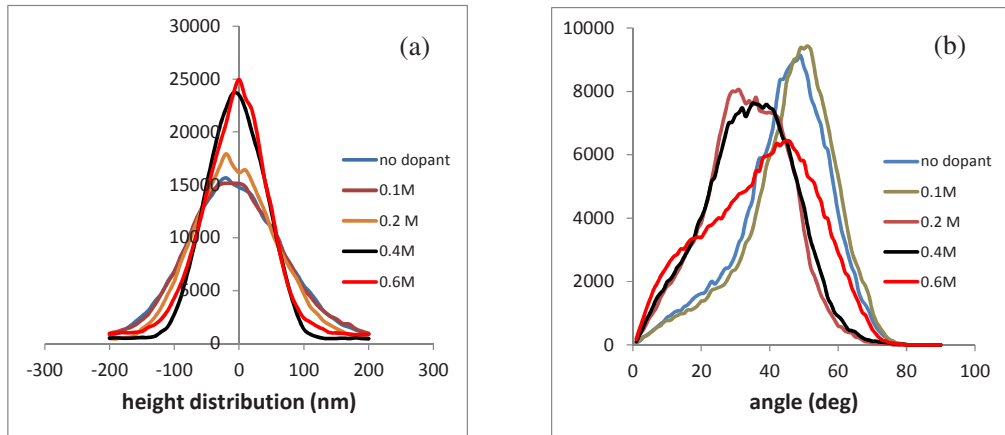


Fig. 2. Histograms of surface features (a) height distribution, (b) angle distribution

For a more quantitative study the AFM image files were processed to study the height variation across the sample surface and the feature angle relative to the substrate. As shown in figure 2a, there was a general narrowing in width of the height histograms at the higher precursor dopant levels, which relates to a reduction in feature height variation. This confirmed the smoothing of the surface shown from roughness measurements and AFM images. For the angle histogram (figure 2b) the trend was less clear showing a narrow angle distribution at un-doped/low dopant levels, then broadening so that the highest dopant level showed a greater spread and lowest selectivity of the surface feature angles. The angle value centring on 50° for the lowest dopant levels and reducing to about 30° for higher doping levels, although at the highest dopant level two main types of feature were suggested with angles around 40° and 10°. This change to lower angle with increased dopant fits again with the increased relative smoothness of the surface.

Electrical measurements, as would be expected, showed an increase in carrier concentration and mobility, with a corresponding decrease in resistivity, as the dopant level increased (figure 3). The mobility initially increased rapidly, before levelling off around 33 cm²/Vs, while the conductivity increases more gradually.

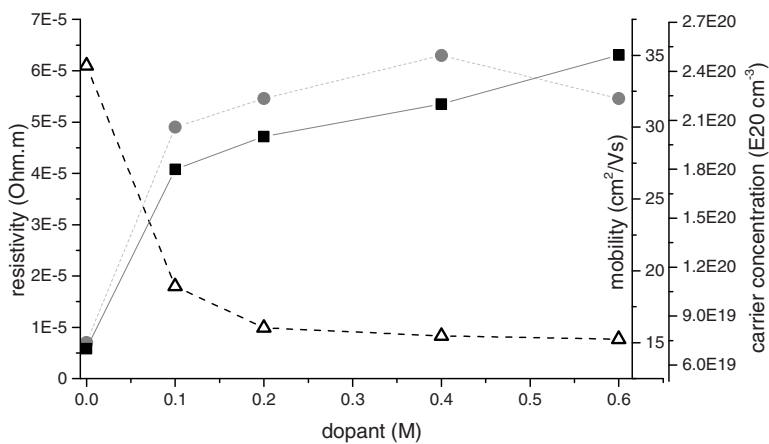


Fig.3. Electrical measurements of the doped samples for carrier concentration, ■, mobility, ● and resistivity, Δ.

The electrical activity of the F depends on it substituting at a lattice site for an oxygen ion and as can be seen the addition of extra F makes less of an improvement to the carrier concentration, so probably reaching the solubility limit of the F in the SnO₂ lattice. These additional electrically inactive dopants may decrease the mobility or at least prevent improvement [15]. Similar behaviour was seen by Oshima *et al*, although their film carrier concentrations were generally higher with much lower mobilities [16].

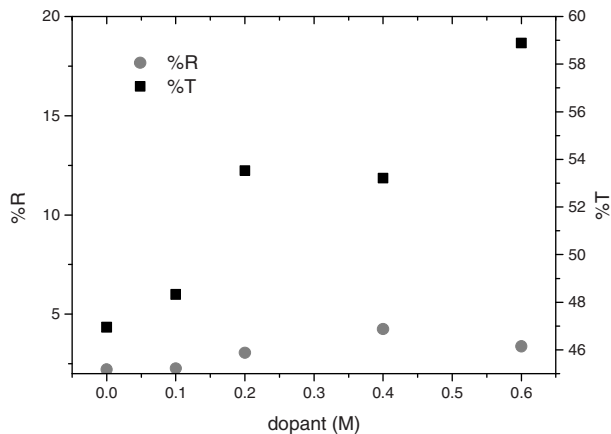


Fig. 4. Graph of average reflectance and transmission between 350 nm and 1000 nm.

The increased carrier concentration would generally be expected to lead to increased free carrier absorption (FCA) and hence a reduction in optical transmission [17]. However, there was actually a small linear increase in the average transmission (figure 4). The average values were calculated over the range 350 nm to 1000 nm. Assuming that the remaining light lost, after accounting for transmission and reflection, was due to absorbance, this would imply a decrease in absorbance with increased dopant levels. Moholkar *et al.* [18] reported an initial increase in optical transmission on doping, which they ascribe to improved crystallinity and a pin-hole free surface. Improved crystallinity of our films on doping, as confirmed by the XRD discussed later in this paper, could also in part explain the increase in transmission seen in our samples. The seemingly low values of the average transmission (62% maximum) relate to both the very thick film (1.8 μm) and that due to the geometry of the spectrophotometer the incident angle was 30° - hence increasing reflectance and reducing transmission. Despite this, maximum transmission values between 64% and 75% were obtained at a wavelength of 800 nm (Figure 5a).

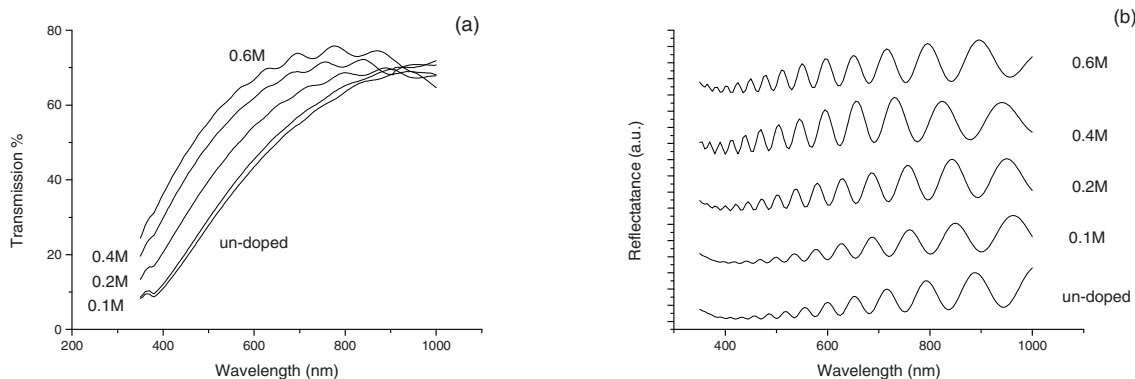


Fig.5. Spectrophotometry measurements for (a) Transmission (absolute values), (b) Reflectance (offset).

As the samples all had similar thickness the reflectance results, shown offset in Figure 5b, all had similar periods. The refractive index is related to the amplitude of the oscillations, which are again similar. As a result, this implies only small differences in the refractive index. The comparatively high film roughness causes the attenuation of the extreme values in all the spectra.

Table II. Calculated crystallite sizes for the SnO₂ films for different precursor doping levels.

Dopant M	[101]	[200]	[211]
	nm		
0		26	24
0.1		22	22
0.2	24	22	24
0.4	21	25	22
0.6	33	34	26

Grain size is another property which can affect the mobility and the associated number of boundaries and traps. However, calculations, via Scherrers formula [19], (Table II) showed little variation in grain size, which was also reported by Shanthi *et al* in their study of SnO₂:F films deposited by spray pyrolysis [20]. The crystallite size is determined from the experimental half-widths of the various peaks, so the error in determination of the grain size will increase for films of lower crystallinity (*i.e.* broader, noisier peaks). This makes it more difficult to accurately determine small changes in grain size.

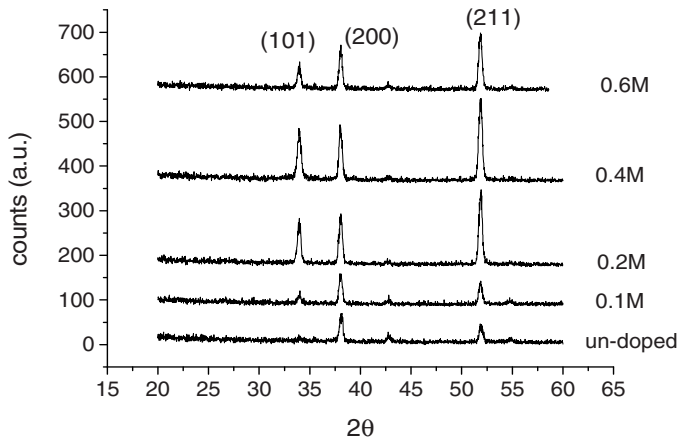


Fig.6 X-ray diffraction of the SnO₂ dopant samples.

The study did show a change in the XRD from non-doped to doped, but no significant changes between the doped samples as shown in figure 6. Other research has also shown changes in orientation between doped and non-doped films [21], but the exact changes depended on the precursor chemistry and deposition conditions. Doping the samples led to increased intensity in the signals at 34° (101) and 52° (211) relative to 38° (200). Overall, as judged qualitatively, there was a reduction in preferential orientation with the three main

diffraction peaks (101), (200) and (211) diffraction peaks becoming closer in intensities. From a doping level of 0.2M (in the precursor) there was an improvement in the crystallinity of the films as shown by the increased intensity, narrowing and reduction in signal/noise levels.

Table III. Electrical properties of selected annealed samples.

Annealing temperature °C	Sheet resistance Ω/sq	Resistivity $\Omega.\text{m}$	Mobility cm^2/Vs	Carrier concentration cm^{-3}
600	18	1.8E-05	26.9	1.3E+20
200	17	1.7E-05	26.2	1.4E+20
25	16	1.6E-05	27.9	1.4E+20

Finally, selected samples were annealed to confirm the stability of APCVD TCO. Samples were annealed at temperatures between 200 °C to 600 °C under a 0.5 l/min flow of air for 1 hour. No change was seen in any of the optical properties (transmission, haze), while the Hall measurements (summarised in Table III) established that no large changes occurred in mobility or carrier concentration. The change in resistivity on annealing is within experimental measurement error.

4. Conclusion

A series of $\text{SnO}_2:\text{F}$ thin films have been deposited under different APCVD F-dopant concentrations. These established increased doping levels led to a decrease in surface roughness along with a reduction in feature size. The surface features also showed a decrease in the average angle, although with a broader distribution. As expected increased doping gave increased carrier concentration and mobility, with a non-linear decrease in resistivity. Interestingly the transmission showed a linear increase with doping level, suggesting a reduction in absorbance (in the visible and very near-infrared range). The polycrystalline structure became less selective in orientation on doping, but no further change was seen on increasing the dopant level. The thermal stability of the films under elevated annealing temperatures was shown to be high, as only marginal changes in electrical and optical properties were detected. This giving yet another reason for use of the APCVD technique.

Acknowledgements

This work was financed by Framework 7 grant FP7 NMP CP-IP 214134-2 N2P “Flexible production technologies and equipment based on atmospheric pressure plasma processing for 3D nano-structured surfaces”.

References

-
- ¹ Gordon, R.G., 2000, MRS Bull. 25, p.52.
 - ² Lewis, B.G., Paine, D.C., 2000, MRS Bull. 25, p.22.
 - ³ Beneking, C., Rech, B., Wieder, S., Kluth, O., Wagner, H., Frammelsberger, W., Geyer, R., Lechner, P., Rubel, H., Schade, H., 1999, Thin Solid Films 351, p. 241.
 - ⁴ Dagkaldiran, U., Gordijn, A., Finger, F., Yates, H.M., Evans, P., Sheel, D.W., Remes, Z., Vanecek, M., 2009, Mater.Sci. Eng.B 159-160, p.6.
 - ⁵ Brook, L.A., Evans, P., Foster, H.A., Pemble, M.E., Sheel, D.W., Steele, A., Yates, H.M., 2007, Surface and Coating Technology, 201, p.9373.
 - ⁶ Yates, H.M., Evans, P., Sheel, D.W., Dagkaldiran, U., Gordijn, A., Finger, F., Remes, Z., Vanecek, M., 2009, Int.J.Nanotechnol. 6, p.816.
 - ⁷ Yates, H.M., Evans, P., Sheel, D.W., Dagkaldiran, U., Gordijn, A., Finger, F., Remes, Z., Vanecek, 2009, ECS Transactions, 25, p.789.
 - ⁸ Yates, H.M., Evans, P., Sheel, D.W., Remes, Z., Vanecek, M., 2010, Thin Solid Films 519, p.1334.
 - ⁹ Volintiru, I., de Graaf, A., van Deelen, J., Poodt, P., 2011, Thin Solid Films 519, p.6258.
 - ¹⁰ Yates, H.M., Evans, P., Sheel, D.W., Nicolay, S., Ding, L., Ballif, C., 2012, Surface and Coatings Technology, 213, p.167.
 - ¹¹ Arefi-Khonsari, F., Bauduin, F., Donsanti, F., Amouroux, J., 2003, Thin Solid Films 427, p.208.
 - ¹² Agashe, C., Hupkes, J., Schope, G., Berginski, M., 2009, Solmat 93, p.1256.
 - ¹³ Zaouk, D., al Asmar, R., Podlecki, J., Zaatar, Y., Khoury, A., Foucaran, A., 2007, Microelectronics Journal, 38, p.884.
 - ¹⁴ Lee, S-Y., Park, B-O., 2006, Thin Solid Films 510, p.154.
 - ¹⁵ Proscia, J., Gordon, R.G., 1992, Thin Solid Films 214, p.175.
 - ¹⁶ Oshima, M., Takemoto, Y., Yoshino, K., 2009, Phys.Status Solidi C6, p.1124.
 - ¹⁷ Fay, S., Steinhäuser, J., Nicolay, S., Ballif, C., 2010, Thin Solid Films 518, p.2961.
 - ¹⁸ Moholkar, A.V., Pawar, S.M., Rajpure, K.Y., Bhosale, C.H., Kim, J.H., 2009, Appl.Surf.Sci. 255, p.9358.
 - ¹⁹ Cullity, B.D., Elements of XRD, Addison-Wesley, 1978.
 - ²⁰ Shanthi, E., Banerjee, A., Chopra, K.L., 1982, Thin Solid Films 88, p.93.
 - ²¹ Ma, H.L., Zhang, D.H., Win, S.Z., Li, S.Y., Chen, Y.P., 1996, Solmat 40, p.371.